Eur. Phys. J. C 49, 81–86 (2007)
DOI 10.1140/epjc/s10052-006-0087-4

THE EUROPEAN PHYSICAL JOURNAL C

Regular Article – Experimental Physics

Femtoscopy in $p+p$ vs. heavy ion collisions in STAR

Z. Chajecki[a] for the STAR Collaboration

Department of Physics, The Ohio State University, 191 W. Woodruff Avenue, Columbus, OH 43210, USA

Received: 8 August 2006 /
Published online: 28 November 2006 –

Abstract. The geometric substructure of the particle-emitting source has been characterized via two-particle interferometry by the STAR collaboration for several energies and colliding systems at RHIC. In heavy ion collisions the $m_{\rm T}$ dependence of femtoscopic radii has been observed for all particle types by several experiments at different collision energies. This dependence has been thought to arise from space-momentum correlations generated by collective flow. On the other hand, there are several reports of a similar $m_{\rm T}$ dependence by experiments measuring elementary particle collisions. Here, quite different physical mechanisms – including resonances, strings, and uncertainty arguments – have been proposed to explain the dependence. Determining the differences or similarities in the space-time physics driving the signal in heavy ion versus $p+p$ collisions requires a direct comparison of $m_{\rm T}$ dependence of the radii. Such a comparison has, until now, been sorely lacking. STAR data allow, for the first time, such a direct comparison between $A+A$, $d+A$, and $p+p$ collisions, at the same energy, measured in the same detector, and using the same analysis techniques. Surprisingly, our preliminary results indicate an $m_{\rm T}$-independent scaling of the femtoscopic radii with overall system size. Possible physics implications of these observations will be discussed, and the importance of long-range non-femtoscopic correlations for low multiplicity collisions will be emphasized.

PACS. 25.75.Gz; 25.75.-q

1 Introduction

Two-particle femtoscopy provides information about the space-time properties of the particle emitting source that allows to understand the dynamics of the system created in high energy collisions by studying the transverse mass dependence ($m_{\rm T}=\sqrt{k_{\rm T}^2+m_\pi^2}$, where $\mathbf{k}_{\rm T}=\frac{1}{2}(\mathbf{p}_{\rm T_1}+\mathbf{p}_{\rm T_2})$) of femtoscopic radii (for the latest review articles see [1–3]).

In this paper femtoscopic results from identical pion interferometry from a small system ($p+p$ collisions) to a large system (Au + Au collisions) measured by the same experiment, at the same collision energy and detector acceptance are presented . The particular focus is on the $m_{\rm T}$ dependence of the femtoscopic radii and an attempt to understand its origins for different initial sizes of the emitting source is made.

2 Analysis details

Particles of interest were reconstructed using the STAR Time Projection Chamber (TPC) [4]. Particle identification was achieved by measuring momentum and specific ionization losses of charged particles in the gas of TPC ($\mathrm{d}E/\mathrm{d}x$ technique). A large data statistics in Au + Au, Cu + Cu and $d+$Au collisions allows to do an analysis for different centralities (impact parameter). In the first two collisions this selection is based on the number of charged tracks at midrapidity, while in $d+$Au collisions the multiplicity within $-3.8<\eta<-2.8$ measured by the forward time projection chamber (FTPC) in the Au beam direction was used to determine the centrality of the collision. Selection of events with a single neutron tagged in the Zero Degree Calorimeter (ZDC) in the deuteron beam direction allows to extract p+Au collisions from $d+$Au data set. However this method introduces a bias in the centrality of the p+Au data sample what causes that most of the events come from non-central collisions. In this study pions with transverse momentum $0.15\,\mathrm{GeV}/c<p_{\rm T}<1.00\,\mathrm{GeV}/c$ were used and the analysis was done for four bins in $k_{\rm T}$ within a range of $[0.15, 0.60]\,\mathrm{GeV}/c$. Two-track effects as splitting (one particle reconstructed as two tracks) and merging (two particles reconstructed as one track) were taken into account in the analysis procedure (see [9] for details).

The dependence of the correlation function on the transverse momentum is studied as a function of three components of pair relative momentum in a Pratt–Bertsch coordinate system [5, 6] in the longitudinally co-moving frame. The fit was performed using a method proposed by Bowler [7] and Sinyukov [8] assuming the Gaussian parameterization of the source (1) [9].

[a] e-mail: chajecki@mps.ohio-state.edu

$$C(Q_{\mathrm{out}}, Q_{\mathrm{side}}, Q_{\mathrm{long}}) = (1-\lambda) + \lambda K(Q_{\mathrm{inv}}) \times \left(1 + e^{-\left(R_{\mathrm{out}}^2 Q_{\mathrm{out}}^2 + R_{\mathrm{side}}^2 Q_{\mathrm{side}}^2 + R_{\mathrm{long}}^2 Q_{\mathrm{long}}^2\right)}\right), \quad (1)$$

where $K(Q_{\mathrm{inv}})$ is the squared Coulomb wave function and λ parameter accounts for contamination like resonance contribution and particle misidentifications.

3 System expansion

This paper is focused mostly on the comparison of low-multiplicity systems with heavy ions. One difference that is expected between large systems such as Au + Au and small systems as $p+p$ and $d+\mathrm{Au}$ is the expansion of the source created in these collisions. This can be studied by the comparison of the initial RMS of the source to the final one. The second value is approximately equal to R_{side} calculated for the lowest k_{T} bin that is $[0.15, 0.25]\,\mathrm{GeV}/c$. The initial RMS of the system cannot be obtained from experimental data so model dependent approach has to be used to estimate it. In this analysis Glauber model was used to calculate this value for nuclei where the proton initial size was taken from an e^- scattering [10] as a reference.

In Fig. 1 the results from $p+p$, $d+\mathrm{Au}$, Cu + Cu and Au + Au collisions at the same energy ($\sqrt{S_{NN}} = 200\,\mathrm{GeV}$) are compared.

The most central Au + Au collisions undergo an expansion by a factor of two while $p+p$ collisions show no or a little expansion. Data points from peripheral $d+\mathrm{Au}$ collisions show similarity like $p+p$ while central $d+\mathrm{Au}$ points exhibit an expansion like in peripheral Cu + Cu. Finally, central Cu + Cu expands like peripheral Au + Au. In this study the smooth expansion of the system from $p+p$ to Au + Au has been observed.

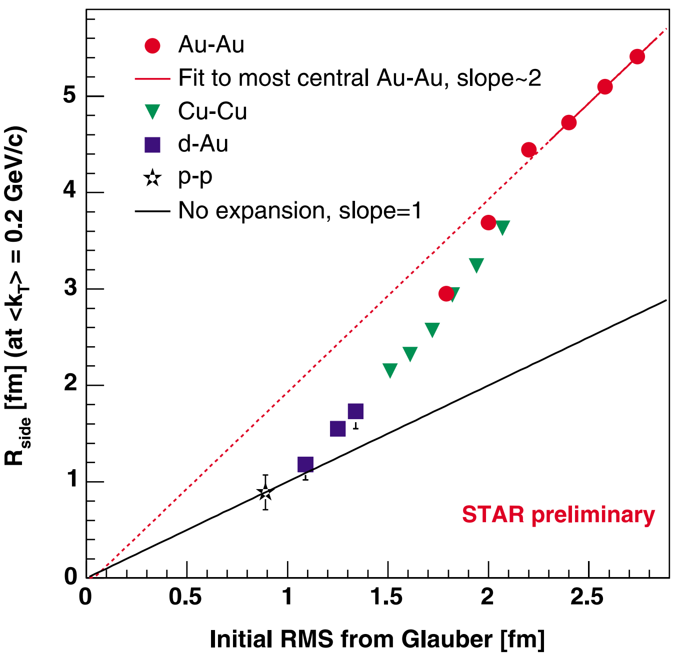

Fig. 1. System expansion: final size of the source vs. initial radii calculated from the Glauber Model. STAR Au + Au data taken from [9]

4 Transverse mass dependence of the femtoscopic radii

4.1 Heavy-ion collisions

In heavy ion collisions a decrease of the femtoscopic radii with an increase of m_{T} is commonly associated with the transverse flow of a bulk matter [9]. In a flow scenario, not only pions but all types of particles should follow approximately "universal" m_{T} dependence [11]. Such dependence for the results from RHIC, AGS and SPS experiments has been presented in [1].

4.2 Low-multiplicity collisions

Naively the transverse flow is not expected in such a small systems as $p+p$ so the natural step would be to check whether this dependence looks different in these systems comparing to heavy ions. If any dependence of the femtoscopic radii is observed then it is crucial to understand its origin. The longitudinal flow is present in $p+p$ collisions however it would affect only R_{long} component of the femtoscopic size of the emission region.

On Fig. 2 the three dimensional radii from $p+p$ and $d(p)+\mathrm{Au}$ collisions are plotted vs m_{T}. For these systems femtoscopic sizes decrease with the increase of the transverse mass and $d+\mathrm{Au}$ results show also the dependence on the centrality similar to results from Au + Au collisions [9].

Additionally, the value of R_{side} and R_{long} for $p+\mathrm{Au}$ collisions is similar to $p+p$ collisions while R_{long} is more like in $d+\mathrm{Au}$ collisions. Comparison of the peripheral $d+\mathrm{Au}$ collisions, that include about 15% of $p+\mathrm{Au}$ collisions, with and without extracted $p+\mathrm{Au}$ events shows no significant difference but that may be due to a fact that the $d+\mathrm{Au}$ sample still includes $n+Au$ events that cannot be excluded from the data.

In elementary particle collisions, resonance production contributes significantly to the m_{T} dependence of the femtoscopic radii [12], while in heavy ion collisions, flow effects dominate this dependence [13]. Other scenarios that can give similar dependence are the Heisenberg uncertainty and the string fragmentation [14].

An alternative explanation of the m_{T} dependence of the femtoscopic radii in $p+p$ collisions at STAR has been suggested by Csörgö *et al.* [15]. Authors using a Buda–Lund hydrodynamic model, that successfully describes the momentum correlations in Au + Au collisions, were able to fit STAR $p+p$ spectra and the femtoscopic radii. But in this case they claim that the transverse mass dependence of the femtoscopic is not due to the transverse flow, but the temperature inhomogeneities of hadron–hadron collisions. The most important implication of this study is that the system created in $p+p$ collisions – like those between Au nuclei – form s a *bulk* system.

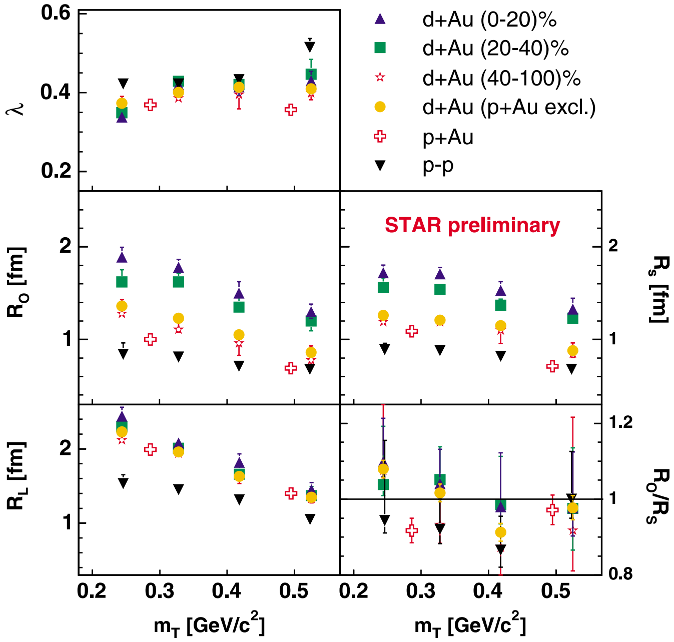

Fig. 2. m_{T} dependence of the femtoscopic radii and λ in $p+p$ and $d(p)+\mathrm{Au}$ collisions at $\sqrt{S_{NN}}=200$ GeV

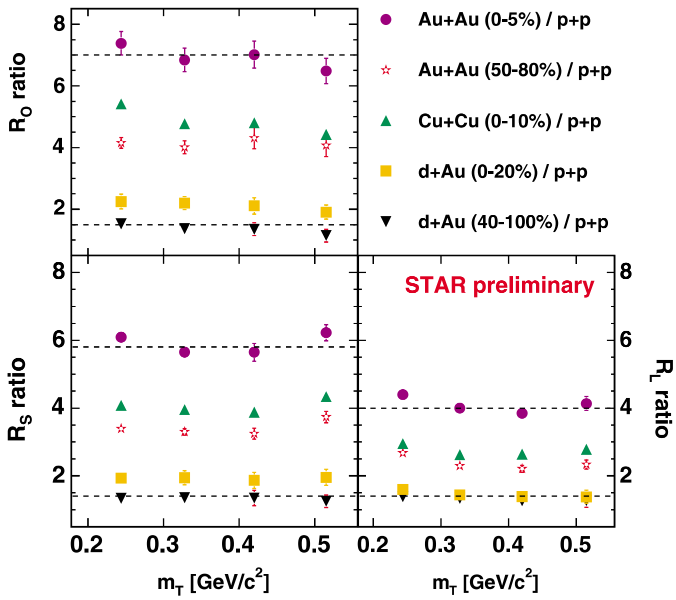

Fig. 3. Ratio of the femtoscopic radii from Au + Au, Cu + Cu and $d+\mathrm{Au}$ collisions at $\sqrt{S_{NN}}=200$ GeV

Non-identical particle correlations like π–K or π–p in Au + Au collisions show a difference in the average emission points of two particles that is due to flow [16]. Therefore, femtoscopic study of particles with different masses in $p+p$ collisions could be used to verify a flow hypothesis in the small systems like $p+p$ and $d(p)+\mathrm{Au}$.

5 Scalings of the femtoscopic radii

5.1 m_{T} scaling

In Sect. 4 the transverse mass dependence of the femtoscopic radii in $p+p$, $d+\mathrm{Au}$ and Au + Au collisions has been discussed. On Fig. 3 the ratios of the three dimensional radii in Au + Au, Cu + Cu and $d+\mathrm{Au}$ collisions to $p+p$ radii are plotted vs. m_{T}. Surprisingly, these ratios look flat although it is expected that different origins drive the transverse mass dependences of the femtoscopic radii in Au + Au and $p+p$ collisions. If these expectations are correct, the data show that one may not distinguish different physics driving $p+p$ and Au + Au collisions when studying pion interferometry.

5.2 Multiplicity scaling

Figure 4 presents the femtoscopic radii dependence on $(\mathrm{d}N_{\mathrm{ch}}/\mathrm{d}\eta)^{1/3}$ ($\mathrm{d}N_{\mathrm{ch}}$ – number of charged particles at midrapidity) for different colliding systems and at different energies of the collisions. The motivation for studying such a relation is its connection to the final state geometry through the particle density at freeze-out. All STAR results, from $p+p$, $d+\mathrm{Au}$, Cu + Cu and Au + Au collisions,

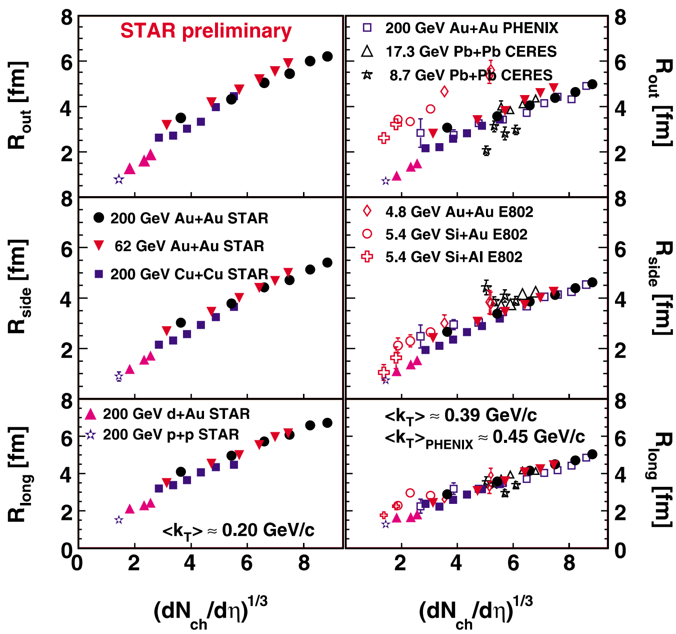

Fig. 4. Femtoscopic radii dependence on the number of charged particles. *Left panel*: results from STAR experiment only for $\langle k_{\mathrm{T}}\rangle \simeq 0.20$ GeV/c; *right panel*: STAR results combined with data from PHENIX, CERES and E802 experiments, mean value of k_{T} is given on the plot

are combined on the left panel of this figure and, as seen, all radii exhibit a scaling with $(\mathrm{d}N_{\mathrm{ch}}/\mathrm{d}\eta)^{1/3}$. On the right panel of this figure STAR radii, this time for different k_{T} range, are plotted together with AGS/SPS/RHIC systematics [1]. It is impressive that the geometric radii (R_{side} and R_{long}) follow the same curve for different collisions over a wide range of energies and, as it was checked, this observation is valid for all k_{T} bins studied by STAR. For the previous study of the multiplicity dependence of the femtoscopic radii see e.g. [17, 18].

Presented results show that the multiplicity is a scaling variable that drives geometric the femtoscopic radii at midrapidity. Because $R_{\rm out}$ includes both space and time information the simple scaling with the final state geometry is not expected. Because of the finite intercepts of the linear scaling [1, 19], results do not confirm predictions that freeze-out takes place at the constant density [20]. This scaling was verified at midrapidity only, and some dependence on rapidity outside this region may be expected [20, 21, 23]; measurements away from midrapidity will be interesting to see whether this "universal" dependence breaks down.

As a result of this study, one can venture to predict the size of the source at midrapidity without knowing anything about the collision (like energy, $N_{\rm part}$, impact parameter, etc.) except for the multiplicity [1, 20, 21]. This scaling is expected to persist for all systems that are meson dominated but is violated for low energy collisions that are dominated by baryons [1, 21, 22].

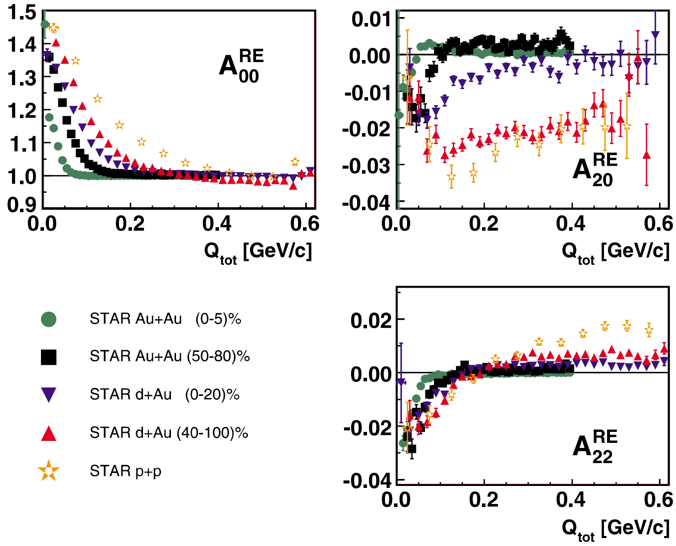

Fig. 5. The first three non-vanished moments of the spherical harmonic decomposition of the correlation function for $p+p$, $d+$Au and Au + Au collisions at $\sqrt{S_{NN}} = 200$ GeV. In all cases $k_{\rm T} = [0.15, 0.60]$ GeV/c

6 Detailed study of the shape of the correlation function at large Q

When doing femtoscopic analysis in low-multiplicity collisions a problem with non-femtoscopic correlations has been observed. It manifests itself as a non-unity tail in the correlation function at large $|\mathbf{Q}|$ whose value depends on the direction of $\mathbf{Q}$. It cannot be removed by the the change of the normalization of the correlation function. In elementary particle collisions [14, 24] these non-femtoscopic correlations were also observed and taken into account by adding different types of *ad-hoc* components to the parameterization of the correlation function. These parameterizations are often explicitly incorrect as they violate symmetry requirements [25].

A common approach to present 3D correlation function is to project it onto the three components of $\mathbf{Q}$ separately. The disadvantage of this approach is that when doing such projections one has to constrain non-projected components to keep a signal but then the full information about the correlation function in the 3D space is lost [26]. To eliminate this inconvenience, a new approach of studying correlations was applied that is based on a decomposition of the correlation function into spherical harmonics (for detailed description of this method see [26]). In this method no cuts are performed on $\mathbf{Q}$'s components and full advantage is taken of symmetries in $\mathbf{Q}$-space to see relevant aspects of 3D correlation functions by looking at 1D plots.

On Fig. 5 the first three non-vanishing moments of the spherical harmonic decomposition of the correlation functions for $p+p$, $d+$Au and Au + Au collisions at the same energy are presented. In the absence of non-femtoscopic correlations, all $A_{l,m}$ moments for $l>0$ should vanish for large $\mathbf{Q}$. However, when looking into the distributions of $A^{\rm RE}_{2,0}$ and $A^{\rm RE}_{2,2}$ on Fig. 5, non-zero structures are observed. The problem does not exists for the most central Au + Au collisions. Some evidence of these non-femtoscopic correlations is seen in the most peripheral Au + Au collisions; they become more important when the size of the source is getting smaller.

The origin of the baseline problem is still under study. However, despite the fact that they are still unknown one can try to parameterize the correlation function for large $\mathbf{Q}$ using the analytical formulas on $A_{l,m}$ components. First, let's start with the formula that is used to calculate $A_{l,m}$ moments from the correlation function.

$$A_{l,m}(|\mathbf{Q}|) = \int_0^{2\pi}\int_{-1}^{1} C(|\mathbf{Q}|, \cos\theta, \varphi) Y^*_{l,m}(\theta,\varphi)\,\mathrm{d}(\cos\theta)\,\mathrm{d}\varphi\,. \tag{2}$$

The problem with the baseline of the correlation function is mostly seen when looking into $A^{\rm RE}_{2,0}$ and $A^{\rm RE}_{2,2}$ moments. In this work the contribution from the other moments is neglected since contributions from other moments are statistically insignificant.

Assuming that the values of $A^{\rm RE}_{2,0}$ and $A^{\rm RE}_{2,2}$ distributions are not changing with $\mathbf{Q}$ one can parameterize these two moments. Using (2) and above assumption one can write the formulas on the correlation function in non-femtoscopic region (see (3) and (4)). Since Lagrange polynomials are orthogonal the parametrization of one moment doesn't affect the other moments.

$$C_{2,0}(|\mathbf{Q}|) = C_{2,0} = \beta\sqrt{\frac{5}{16\pi}}(3\cos^2\theta - 1)\,, \tag{3}$$

$$C_{2,2}(|\mathbf{Q}|) = C_{2,2} = \zeta\sqrt{\frac{15}{32\pi}}\sin^2\theta\cos 2\varphi\,, \tag{4}$$

$$C(\mathbf{Q},\cos\theta,\varphi) = (1-\lambda) + \lambda K(Q_{\rm inv}) \times \left(1 + e^{-|\mathbf{Q}|^2\left(\sin^2\theta\left(R^2_{\rm out}\cos^2\varphi + R^2_{\rm side}\sin^2\varphi\right) + R^2_{\rm long}\cos^2\theta\right)}\right)$$

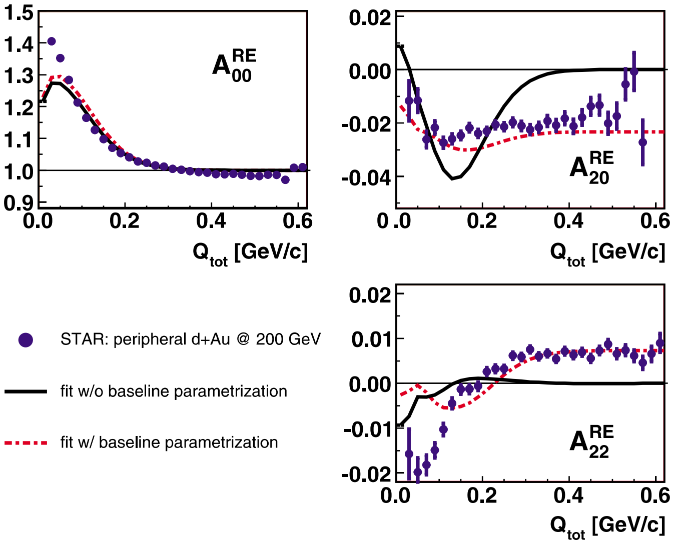

Fig. 6. First three non-vanished components of the spherical harmonic decomposition of the correlation function for peripheral $d+$Au collisions at STAR at $\sqrt{S_{NN}}=200$ GeV; *black curve* – fit to experimental correlation function using(1); *red dotted curve* – fit to experimental correlation function with baseline parametrization. See text for more details

$$+\beta\sqrt{\frac{5}{16\pi}}(3\cos^2\theta-1)+\zeta\sqrt{\frac{15}{32\pi}}\sin^2\theta\cos 2\varphi\,. \quad (5)$$

Here, the new parameters β and ζ represent the constant values of $A^{\mathrm{RE}}_{2,0}$ and $A^{\mathrm{RE}}_{2,2}$, respectively. well as 1D projections of 3D correlation function. Figure 6 shows an example of the fit without baseline parameterization (1) – black solid line – and the fit with baseline parameterization (5) – red dotted line – to the most peripheral $d+$Au collisions in STAR for $k_{\mathrm{T}}\in[0.15, 0.60]$ GeV/c. New fit that accounts for the non-vanished structure of $A^{\mathrm{RE}}_{2,0}$ and $A^{\mathrm{RE}}_{2,2}$ moments has been performed for $p+p$ and $d+$Au data for all studied k_{T} bins. As a result of this work it was noticed that the radii in $p+p$ and $d+$Au collisions are changed up to 10% the most. However the m_{T} scaling described in the section Sect. 5.1 persists as presented on Fig. 7.

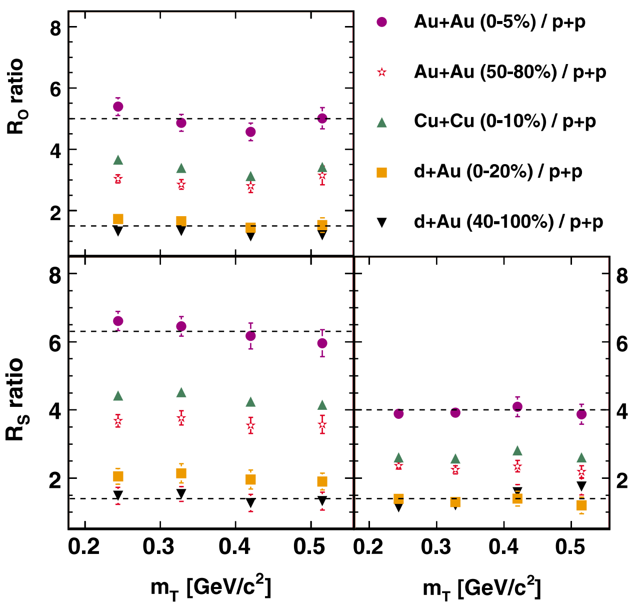

Fig. 7. Ratio of the femtoscopic radii from Au$+$Au, Cu$+$Cu and $d+$Au collisions at $\sqrt{S_{NN}}=200$ GeV. The parameterization of the baseline of the correlation function (5) in the low multiplicity collisions has been taken into account in a fit procedure

7 Conclusions

The results of pion interferometry for all energies and colliding systems at RHIC have been presented. In agreement with data at SPS and AGS, STAR results indicate that the multiplicity is the scaling variable that determines the size of the source at freeze-out. Perhaps surprisingly, the m_{T} dependence of the femtoscopic radii appears to be independent of collision species or multiplicity. The results from the same energy for different collisions show that the system expands by a factor of two for the most central Au$+$Au collisions and at most a little expansion is observed for $p+p$ collisions. Finally, a problem with the baseline of the correlation function for low multiplicity collisions has been reported, and a promising tool based on the spherical harmonic decomposition of the correlation function has been used in order to address it. The physics of this structure remains under investigation.

References

1. M. Lisa, S. Pratt, R. Solz, U. Wiedemann, Annu. Rev. Nucl. Part. Sci. **55**, 357 (2005)
2. T. Csörgö, nucl-th/0505019
3. S.S. Padula, Braz. J. Phys. **35**, 70 (2005)
4. M. Anderson et al., Nucl. Instrum. Methods A **499**, 659 (2003)
5. S. Pratt, T. Csörgö, J. Zimanyi, Phys. Rev. C **42**, 2646 (1990)
6. G. Bertsch, Nucl. Phys. A **498**, 173c (1989)
7. M.G. Bowler, Phys. Lett. B **270**, 69 (1991)
8. Y.M. Sinyukov et al., Phys. Lett. B **432**, 249 (1998)
9. STAR Collaboration, J. Adams et al., Phys. Rev. C **71**, 044 906 (2005)
10. I. Sick, Eur. Phys. J. A **24**, 65 (2005)
11. F. Retiere, M.A. Lisa, Phys. Rev. C **70**, 044 907 (2004)
12. R.M. Weiner, Phys. Rep. **237**, 249 (2000)
13. U.A. Wiedemann, U. Heinz, Phys. Rev. C **56**, 3265 (1997)
14. G. Alexander, hep-ph/0302130.
15. T. Csörgö, M. Csanád, B. Lörstad, A. Ster, hep-ph/0406042
16. STAR Collaboration, J. Adams et al., Phys. Rev. Lett. **91**, 262 302 (2003)
17. M. Gazdzicki et al., Nucl. Phys. A **590**, 197c (1995)
18. B. Tomasik, U.A. Wiedemann, hep-ph/0210250
19. PHENIX Collaboration, S.S. Adler et al., Phys. Rev. Lett. **93**, 152 302 (2004)

20. T. Csörgö, L.P. Csernai, Phys. Lett. B **333**, 494 (1994)
21. R. Stock, Ann. Phys. **48**, 195 (1991)
22. CERES Collaboration, D. Adamova et al., Phys. Rev. Lett. **90**, 022 301 (2003)
23. M.A. Lisa, nucl-ex/0512008
24. NA22 Collaboration, N.M. Agababyan et al., Z. Phys. C **71**, 405 (1996)
25. STAR Collaboration, Z. Chajęcki, AIP Conf. Proc. **828**, 566 (2006) [nucl-ex/0511035]
26. STAR Collaboration, Z. Chajęcki et al., nucl-ex/0505009